N94-30627

209934

P-24

A Toy Model for Estimating N_2O Emissions from Natural Soils

Inez Fung

Introduction

Nitrous oxide is present in the atmosphere in minute quantities. Its concentration in 1988 was ~307 parts per billion by volume (ppbv), about a thousand times less than that of CO_2, and it is increasing at the rate of ~0.8 ppbv/yr (Elkins et al., in press). The seemingly small growth rate, ~0.25%/yr, is the result of a large imbalance (~30%) between the sources and sinks.

Despite its low abundance in the atmosphere, N_2O plays an important role in the radiative and chemical balance of the atmosphere. The extremely long lifetime of N_2O, ~150 years, means the system has a very long memory of its emission history. The radiative forcing of N_2O, molecule for molecule, is ~200 times that of CO_2 (Houghton et al., 1990). N_2O is destroyed in the stratosphere by photolysis and by reaction with electronically excited oxygen atoms [$O(^1D)$], making it the dominant precursor of odd nitrogen (NO_x) in the stratosphere. Thus an increase in N_2O would lead to an increase in stratospheric NO_x, which would catalyze the destruction of stratospheric ozone.

The sources of N_2O are not well known. Of the ~15 Tg N (1 Tg = 10^9 kg) produced annually, by far the largest source seems to be emissions from natural soils, 6 ± 3 Tg/yr, followed by emissions from the oceans, 2 ± 1 Tg/yr (Seiler and Conrad, 1987). The strength of these natural sources is estimated from only a handful of flux measurements. Other sources include emission from combustion, biomass burning, and agricultural fields amended with nitrogenous fertilizers. For some time, it was thought that, like CO_2, the primary cause for the increasing trend was combustion of fossil

fuels, in particular, coal-burning power plants producing electricity (Hao et al., 1987). However, recent identification of an artifact in the flask sampling procedure ruled out combustion (including biomass burning) as the major cause of the N_2O trend (Muzio and Kramlich, 1988). We do not know why N_2O is increasing in the atmosphere.

Global models of the N_2O cycle (e.g., Prinn et al., 1990) use variations in the concentrations of N_2O in the atmosphere to infer the location and magnitude of the N_2O sources and sinks. The results point to large source(s) located in the tropics that contribute significantly to the latitudinal gradient and secular trend of N_2O in the atmosphere. Such an approach, however, cannot distinguish among individual sources without direct information about at least some of the sources and sinks themselves.

In a separate paper (Bouwman et al., in preparation), we focused, not on the N_2O budget itself, but on the largest single source term in the budget, i.e., emissions from natural soils. The effects of fertilizer application and other human perturbations on the N_2O emissions from soils were not considered. A very simplistic model was developed for estimating directly the geographic and seasonal variations of N_2O emissions from natural soils. We hope that the model, and the sensitivity studies using it, will provide guidance for measurement strategies to reduce systematically uncertainties about this single source. The source distribution may also be a useful input to two-dimensional and three-dimensional models to test hypotheses about the N_2O budget. The reader is referred to Bouwman et al. for a detailed description of the data, model, and sensitivity analyses. Here, we present an account of the assumptions and decisions involved in the construction of the model.

A Conceptual Model of N_2O Production

N_2O is produced by both nitrification and denitrification. Denitrification occurs under oxygen limiting conditions. Nitrogenous oxides, principally nitrate (NO_3^-) and nitrite (NO_2^-), are reduced to dinitrogen gases (N_2), nitrous oxide, and nitric oxide (Firestone and Davidson, 1989). Under strictly anaerobic conditions nitrous oxide and nitric oxide (NO) may also be used as electron acceptors. In nitrification, ammonia (NH_4^+) is oxidized to NO_2^- or NO_3^-. In natural soil ecosystems, the NH_4^+ comes from decomposition and mineralization of organic matter only. The reader is referred to Bowden (1986) for a review of the biogeochemistry and measurements of N_2O production in undisturbed ecosystems.

Consider a conceptual model of N_2O production in a unit area of unperturbed land with a given vegetation/soil complex. Litterfall

associated with vegetation cycles supplies fresh organic matter to the soils. The organic matter is decomposed and mineralized by microbial activity, thus delivering N for nitrification and denitrification. The decomposition rate is regulated by soil temperature and other parameters of the soil environment. Under most soil conditions, both nitrifying and denitrifying bacteria are active. The relative contribution of N_2O produced via the nitrification and denitrification pathways is determined largely by the degree of water saturation and aerobicity of the soils. The wetter the soil, the lower the oxygen content and the more likely denitrification processes are to dominate. Soil water and oxygen status are, in turn, governed by the net water supply at the surface, soil water-holding capacity, and drainage properties. Other inherent soil properties, such as pH and fertility, also modulate the microbial activity and N_2O production.

The controls on N_2O production from natural soils can be summarized as (1) carbon and nitrogen availability, (2) temperature, (3) soil moisture, (4) soil oxygen status, (5) soil fertility, and (6) soil pH. Because global data on soil pH are of questionable quality, this factor was not included in our analysis.

Global Data for the Toy Model of N_2O Production

We now present a synthesis of our conceptual understanding of the controls on N_2O fluxes into a quantitative framework, i.e., into a model. The ultimate objective of the model is to evaluate what contribution natural ecosystems make to the global N_2O budget and how the contribution would change with global change. Given the paucity of measurements, our immediate goal is to test the conceptual model of N_2O fluxes and identify gaps where measurements and analyses are needed.

The focus of the model requires data or inputs that must be global in domain and span at least a year. The primary gridded data sets available are described below:

- *Soils:* The 1:5M FAO/Unesco soil maps (1971–1982, 1974, 1988) include information on dominant soil units, associated soils (when they cover at least 20% of the area) and inclusions, texture of the dominant soil, and slope. We used information on the major soil units (106) and texture of the topsoil (upper 30 cm) from the data digitized at $1° \times 1°$ resolution for the globe by Zobler (1986). The spatially dominant soil units in the $1°$ grid cell were recorded.

  Texture reflects the relative proportions of clay (particles less than 2 μm in size), silt (2–50 μm), and sand (50–2000 μm). Three tex-

ture classes for the topsoil are distinguished in the FAO soil maps: coarse, medium, and fine. At 1° resolution, a spatially dominant texture cannot always be established. And so, four other texture classes were included in the digital data base: coarse/medium, coarse/fine, medium/fine, and coarse/medium/fine. Furthermore, texture information was not available everywhere in the FAO soil maps, in particular for some of the organic soils, e.g., Histosols. A separate class, "organic," was added to the texture description. These additional five classes composed <10% of the land surface.

The soil type information is used to translate directly into fertility and drainage, while the type and texture information are used to derive soil storage capacity. These are described briefly below and in detail in Bouwman et al. (in preparation). Figure 1 shows the global distribution of soil texture, grouped into six classes.

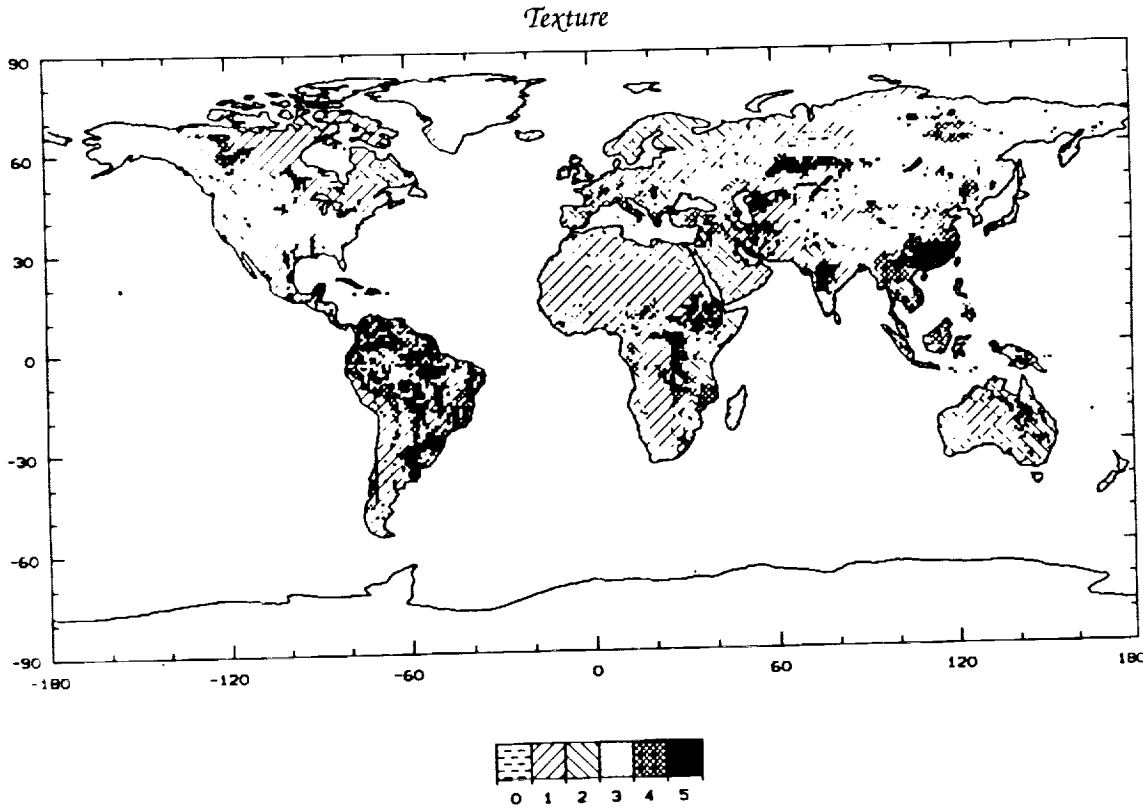

Figure 1. Distribution of soil texture: 0 = organics, 1 = coarse, 2 = coarse/medium, 3 = medium, 4 = medium/fine, 5 = fine. Spatial resolution is 1° × 1°.

- *Vegetation:* The satellite-derived normalized difference vegetation index (NDVI) is a measure of primary productivity of the vegetation. The NDVI is the difference between the radiances in the visible (0.58–0.68 μm) and near-infrared (0.725–1.1 μm) wavelengths, normalized by the sum of the radiances. The radiances are measured by the advanced very high resolution radiometer (AVHRR) on board the NOAA series of polar-orbiting satellites (Tarpley et al., 1984). In this study, monthly NDVI composites for 1984 were gridded at 1° × 1° resolution for the globe, and then summed to produce the annual total. Although a digital data base of vegetation types exists (Matthews, 1983), vegetation information is used only for verifying measurement site characteristics and for analysis of model results.
- *Climate:* Shea (1986) has produced climatologies of monthly mean surface air temperature and precipitation, at 2° × 2° resolution for the globe, from the available station observations. In the conceptual model, the climate parameter important for N_2O production is soil temperature. Lacking a global climatology for soil temperature, we used surface air temperatures instead. This would introduce phase errors, of up to a season in middle and high latitudes, in the seasonality of N_2O production.

The finest spatial resolution of these data sets is 1° latitude by 1° longitude, so that there are ~15,000 grid cells for the ice-free land surface. The climate data are monthly means. With this resolution, the model cannot resolve episodic effluxes of N_2O after rainstorms and spatial "hot spots" which are often reported. The importance of such high-frequency, local events in the global budget has not been established. The model must parameterize, in some way, their integrated effect, and evaluate their contribution to the global annual flux.

A Toy Model for N_2O Production

Fluxes of N_2O from temperate grasslands have been extensively modeled based on the comprehensive measurements there (e.g., Parton et al., 1987, 1988). For the other soil types around the globe, there is a dire lack of N_2O flux measurements, let alone quantitative relationships between N_2O fluxes and the various controlling parameters. We do not know if the relationships established for grasslands can be extrapolated elsewhere.

Our strategy for the toy model for N_2O production is to first translate ideas about relative importance of each of the controlling parameters into ranked nondimensional indices. The indices are scaled

from 0 to 10, or from 0 to 5, with high numbers signifying importance for N_2O production and 0 signifying no production. Our choice of a scale of 5 or 10 depends on the number of levels we think we can discriminate within the scale.

Using nondimensional variables to denote relative importance is not a new concept. It was employed, for example, to represent temperature and moisture controls in the N_2O model of Mosier and Parton (1985). Such a translation is straightforward for numeric data such as temperature. In this toy model, we also created nondimensional scales for ordinal data such as fertility and drainage by carrying out a subjective ranking of soil units and texture information. The control indices are then combined to form the index for N_2O fluxes. Comparison of the scaled nondimensional N_2O fluxes with field measurements provides an evaluation of the validity of the model and, one hopes, an algorithm for calculating N_2O fluxes from the scaled variables.

The model is illustrated schematically in Figure 2. A central part of the problem is to model how soil water regulates the degree of nitrification/denitrification and hence N_2O production. A bucket model of water balance is used. The bucket model takes into account differences in soil drainage and topsoil texture and determines the water and oxygen status of the topsoil. For both nitrification and denitrification, N_2O flux is also proportional to the amounts of carbon and nitrogen available in the soil, the rate of mineralization of the carbon and nitrogen, and soil fertility.

With this approach, we need to derive the global distribution of the five major regulators of N_2O production. Three of them vary monthly: decomposition of soil organic matter (SOD), water availability (WATER), and oxygen limitation (OXYGEN); the remaining two, soil fertility (FERT) and carbon and nitrogen availability (CARBON), are constant through the year. Below, we describe in detail the derivation of each of the regulators and their synthesis to yield the nondimensional N_2O flux.

Soil Carbon and Nitrogen Available

Litterfall and root decay are the major sources of carbon and nitrogen to the soil. For most ecosystems, there is an abundance of litter on the ground throughout the year. Hence the seasonal variation of C and N mobilization in the litter is generally governed by decomposition rates rather than by seasonal variations in litterfall. Here we assumed that geographic pattern of annual litterfall is the same as that of annual net primary productivity of the ecosystems, for which the satellite-derived NDVI has been shown to be a good correlate (Goward et al., 1986; Box et al., 1989). Because litterfall is

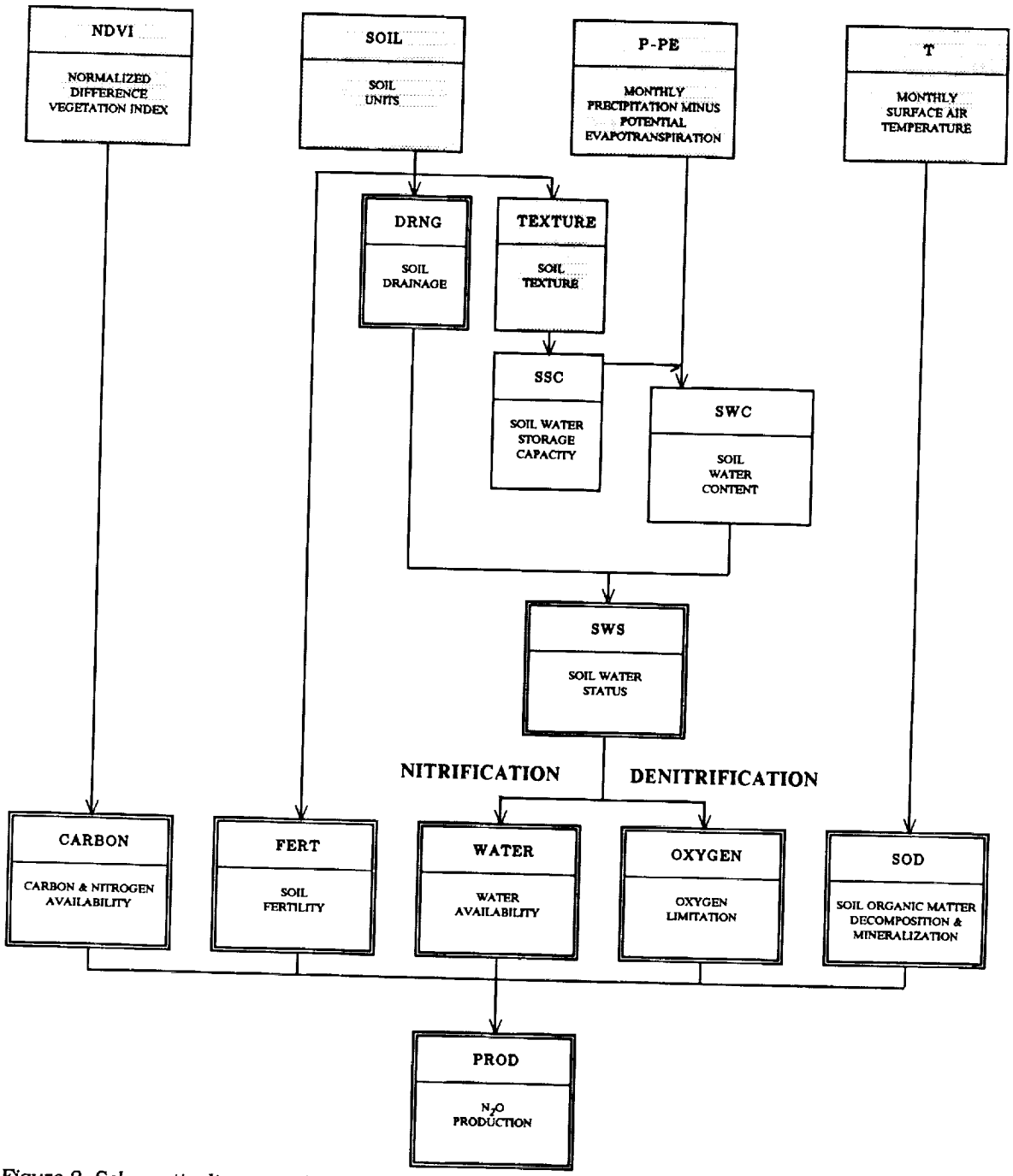

Figure 2. Schematic diagram of the toy model of N_2O production. Shaded boxes denote input data and double-bordered boxes denote nondimensional indices.

not in phase with productivity, the annual NDVI totals, rather than NDVI for individual months, were used.

Monthly NDVI values range from -0.1 to 0.5, and the annual totals range from -0.1 to 4. To be consistent with the other factors used in the study, these NDVI totals were, in turn, rescaled to range from 0 to 10 to obtain the index CARBON (Figure 3). We note that we could have used, instead of the NDVI, a global distribution of net primary production (NPP) obtained by assigning literature values of annual NPP to the digital data base of vegetation. The use of the NDVI captures the variability of NPP within each vegetation type, at the same resolution as the soil data.

Delivery of Nitrifiable N

The rate of carbon and nitrogen delivery is governed by the rate of decomposition and mineralization of soil organic matter, which are regulated by soil temperature, soil moisture, soil fertility, and soil texture. Here, we introduced a factor in the model to represent the

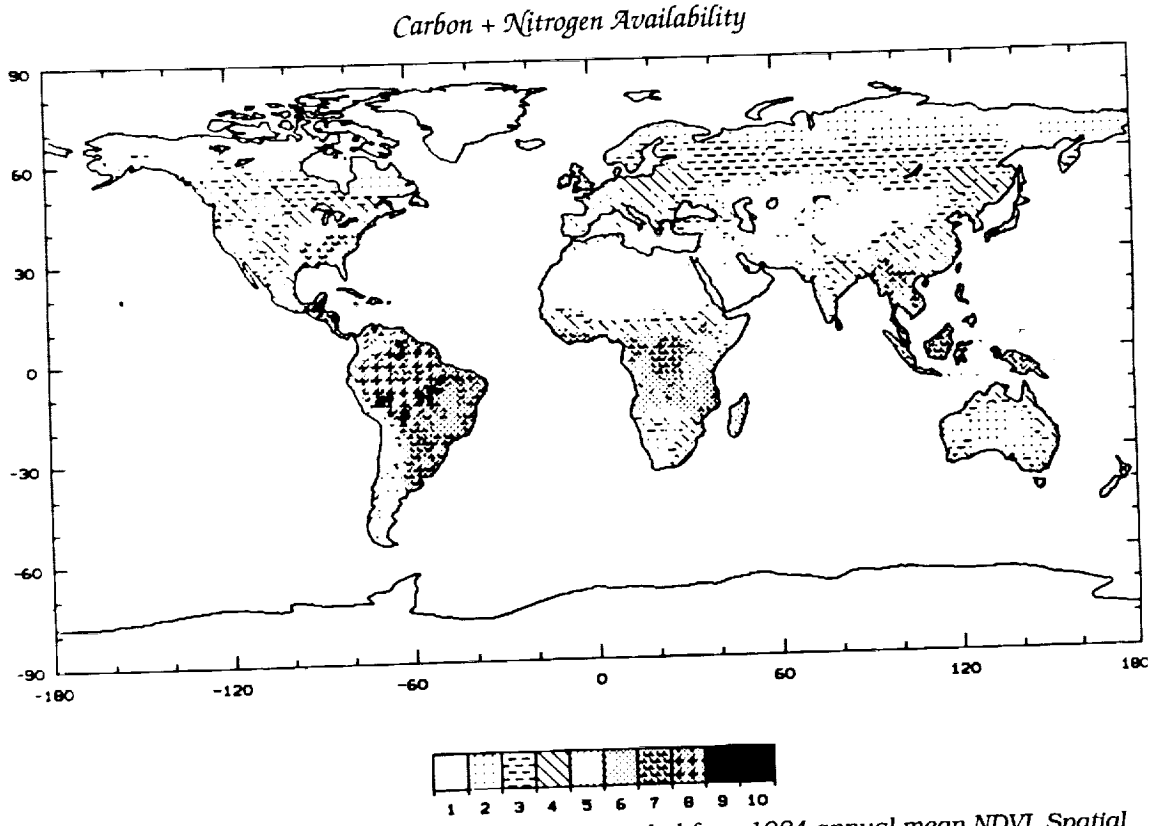

Figure 3. Global distribution of the index CARBON, scaled from 1984 annual mean NDVI. Spatial resolution is 1° × 1°.

temperature effect on the supply of nitrogen and carbon through decomposition of organic matter (SOD).

Three temperature dependencies for the factor SOD were investigated (Figure 4). The first (referred to as SOD1) is an exponential function describing the temperature effect on N_2O fluxes obtained for semiarid grasslands (Mosier and Parton, 1985; Parton et al., 1988). SOD1 = 10 at T = 50°C, and SOD1 = 0 for T ≤ 0°C, with a rapid increase between 10 and 30°C. The second equation (referred to as SOD2) is a quadratic function adapted from Parton et al.'s (1988) equation for N_2O fluxes from grasslands. The optimum (SOD2 = 10) is at T = 35°C. To avoid negative values, SOD2 was set to zero at T < 7°C and T > 50°C. The third relationship tested (referred to as SOD3) is a set of linear functions for four broad ecosystem groups: broad-leaved vegetation, needle-leaved vegetation, grasslands, and tropical vegetation. The functions were derived from observations of CO_2 evolution from soils (Fung et al., 1987). They were set to SOD3 = 10 at T = 50°C. The different slopes of the four functions reflect the differences in litter composition for the broad biome groups. For comparable temperature ranges, grasslands, having a higher fraction of easily decomposed material in its detritus than needle-leaved woody vegetation, would have a faster relative decomposition rate. The maximum

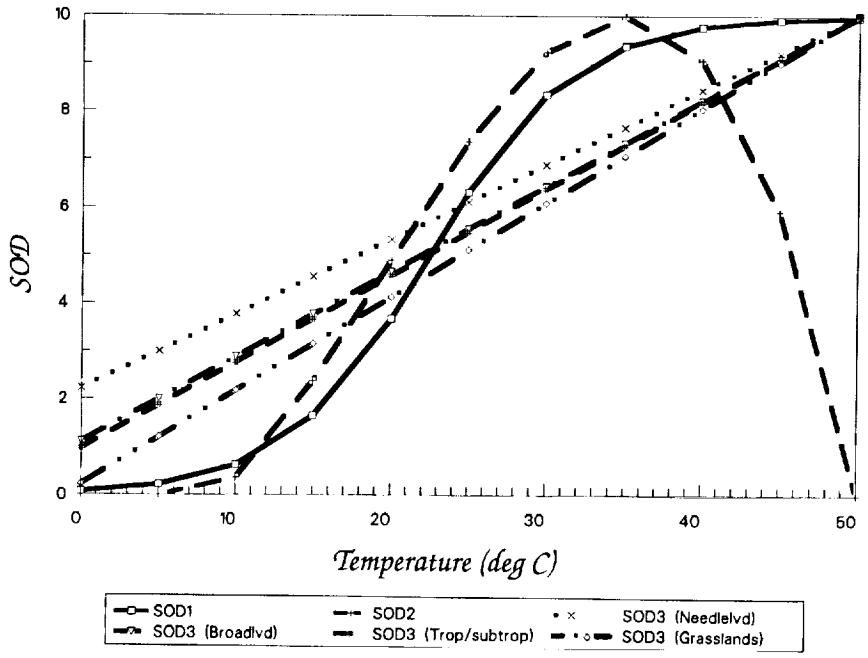

Figure 4. Index of the rates of soil matter decomposition (SOD) as a function of temperature.

values at T = 50°C do not capture the adaptation of microbes to their environmental conditions.

We used the exponential curve (SOD1) in the reference formulation for N_2O production (see "N_2O Production" below).

Soil Water and Oxygen Status

A key to distinguishing the pathways of nitrification vs. denitrification is the degree of saturation and aerobicity of the soil, which is, in turn, determined by the soil drainage properties, as well as by the amount of water present in the topsoil vs. the maximum amount of water allowed in the topsoil, i.e., the soil water storage capacity (SSC).

A first step in modeling the water balance of the topsoil is the determination of the soil water storage capacity. SSC is the total amount of water held in the upper 30 cm of the soil profile at field capacity (soil water potential of 10 kPa), after internal drainage and redistribution have ceased. Global distributions of SSC are used in general circulation models (GCMs); recent hydrology schemes assign SSC based on vegetation and/or soil characteristics. We prescribed SSC based on soil texture for most soils. SSC is 120 mm, 80 mm, and 40 mm for fine-, medium-, and coarse-textured soils, respectively. For a number of soils, covering about 30% of the ice-free land surface, properties other than texture exert the primary influence on water retention; their SSCs were assigned without regard for texture. Generally, these are fine-textured Ferralsols and Vertisols whose aggregates and swell-shrink properties, respectively, reduce their water-holding capacity to that of medium-textured soils. The global distribution of SSC is shown in Figure 5.

Soil Water Budget Model

The change in soil water content (SWC) is the difference between the supply and demand of moisture at the surface. Supply is governed to a large extent by precipitation, while demand is governed by evaporation through soils and transpiration through plants. Runoff (on sloping land) or ponding (on level land) occurs when the net input of water plus the initial amount of soil water exceed soil water storage capacity after drainage has been accounted for.

There are several soil moisture models used in general circulation models, ranging from the simple bucket model of Manabe (1969), where SSC was uniformly 15 cm, to the simple biosphere model (SiB) of Sellers et al. (1986) and the complex biosphere-atmosphere transfer scheme (BATS) of Dickinson (1984) and Dickinson et al. (1986), which take into account the effects of biome differences on soil water balance. Not only do these recent models distinguish among soil evaporation and plant evaporation and transpiration,

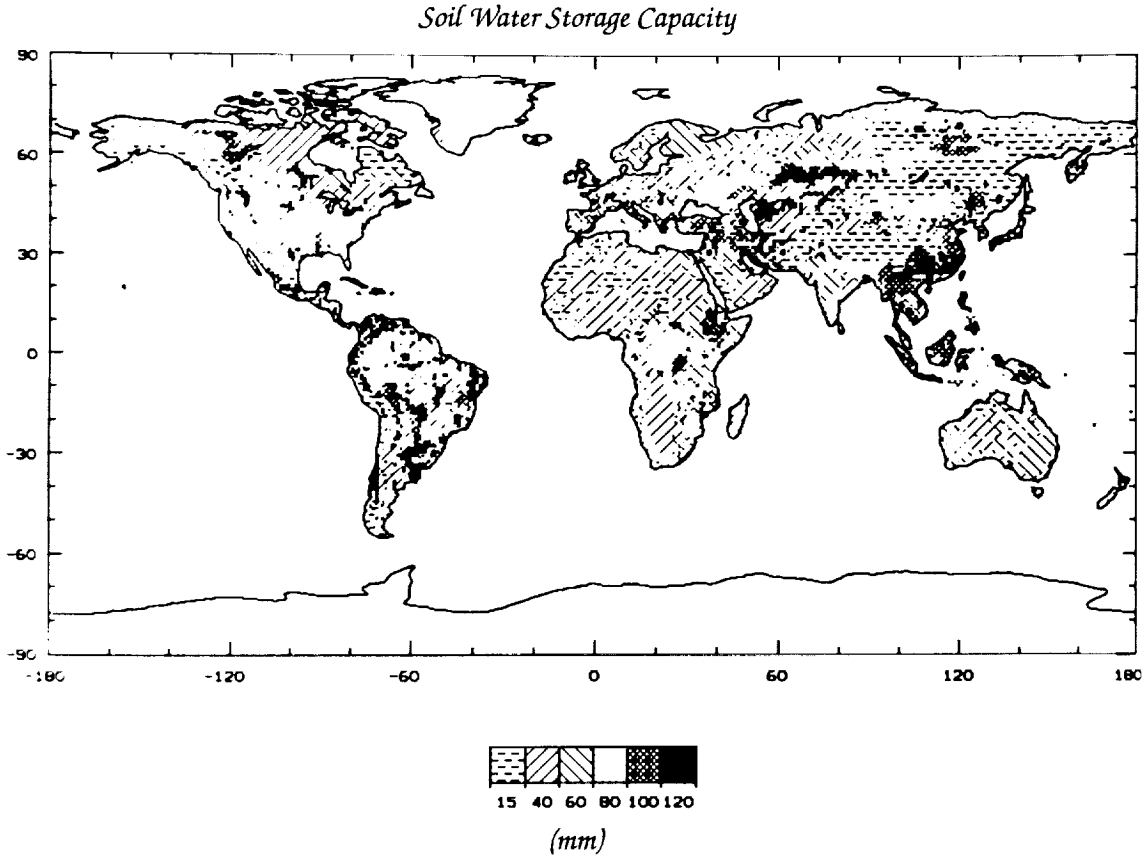

Figure 5. Distribution of SSC.

they also model explicitly vertical profiles of moisture in the soil. These recent models are not yet fully validated in GCMs and are too complicated for the toy model at hand. However, in a simple bucket model where supply and demand are independent of soil moisture itself, the solution to the soil moisture equation is not uniquely determined; it is dependent on the initial SWC assumed, unless the SWC = 0 or SWC = SSC (runoff) sometime during the year.

In this study, we chose a soil moisture model that is simple in design, and whose solution is not dependent on an arbitrarily chosen initial condition. We adapted the Mintz and Serafini (1981) model for the calculation of the monthly soil water content (SWC_m). In this model, net supply is the difference between monthly precipitation (P_m) and evaporation from wet canopies (EI_m), while demand is the sum of transpiration through plants and evaporation from soils (ETS_m). The time step of a month corresponds to the time resolution of the global precipitation climatology used.

$$SWC_m = SWC_{m-1} + (P_m - EI_m) - ETS_m$$

Potential evaporation (PE_m), a measure of the maximum demand for moisture by the atmosphere, was calculated from the surface air temperature according to Thornthwaite (1948). Mean monthly surface air temperatures (T_m) and precipitation (P_m) were obtained from the climatologies compiled by Shea (1986). For simplification, precipitation in the form of snow was treated as rainfall. Three moisture regimes were considered, dependent on the relation between P_m and PE_m:

$P_m = 0$ $\quad EI_m = 0$, $\quad ETS_m = PE_m \times \beta_m \times \alpha$

$P_m < PE_m$ $\quad EI_m = P_m$, $\quad ETS_m = (PE_m - P_m) \times \beta_m \times \alpha$

$P_m \geq PE_m$ $\quad EI_m = PE_m$, $\quad ETS_m = 0$

where

$$\alpha = 0.4$$

and

$$\beta_m = 1 - e^{-\gamma\left[\{SWC_{m-1} + (P_m - EI_m)/2\}/SSC - \delta\right]}$$

The coefficient α expresses the ratio of the amount of water extracted from the topsoil to the extraction from the full rooting zone (as noted before, we consider only the topsoils). The function β describes the maximum water extraction as a function of soil water content and soil characteristics. Its parameter γ depends on topsoil texture and mineralogy, while δ represents the water unavailable to plants, i.e., the intercept of the water extraction curve β. The values of δ and γ are dependent on soil texture (see Bouwman et al., in preparation). For fine textured soils, $\gamma = 6$, resulting in a strong decrease in water extraction below SWC/SSC $\approx$ 50%. Due to the selected value of δ for clays, water extraction at SWC/SSC < 10% is reduced. In sands and medium-textured soils β sharply declines at values of SWC/SSC of about 40% and 20%, respectively. Because SWC is a function of β, the monthly equilibrium SWC is achieved independently of the initial water content at the start of the simulation.

Effects of Drainage

In the calculation of the soil water content of the topsoil described above, drainage properties of the soil were not considered. Drainage

determines how excess water is removed from the soil, and it is also an indicator of the soil aeration. We ranked the soil drainage index DRNG based on soil texture and other soil properties, with a high rank favoring N_2O production. The very poorly drained soils (DRNG = 5) include those soil groups strongly influenced by groundwater, i.e., Gleysols and Histosols, as well as soils with permafrost within 200 cm of the soil surface (gelic soil units). Freely drained soils, such as Xerosols and Yermosols, occurring in deserts, were assigned a drainage rank of 1. The distribution is shown in Figure 6.

We are uncertain how to model quantitatively the effects of drainage on soil water content. Adding diffusion at the base of the "bucket" may be an appropriate approach, but the values of the diffusion coefficients for different drainages are not well known. Here, we introduced the factor soil water status (SWS), an index of the soil water saturation when drainage effects are considered (Table 1). It is clear that the highest SWS rank of 10 would be assigned to a poorly drained soil when the monthly soil water content SWC is close to the storage capacity SSC of the soil. It is not clear how to rank the intermediate values of drainage and SWC/SSC. We noted several points: (1) Distinguishing saturation levels <20% is not important, so that the SWC/SSC scale can be divided into ten levels as shown. (2) We linearly increased the SWS scale up the saturation scale. (3) We filled in the rest of the table by assuming that N_2O production would likely be asymptotic at high saturation and poor drainage. There is thus much arbitrariness in the SWS scale. It nevertheless represents a first attempt at quantifying our descriptive understanding of the effects of soil drainage characteristics on soil moisture.

Nitrification and Denitrification Potentials

It remains to describe the effects of soil water status on oxygen supply in the soils, i.e., on nitrification and denitrification. Two factors, water availability (WATER) and oxygen limitation (OXYGEN), were derived as indices for nitrification and denitrification potentials, respectively. These two indices are based on the two moisture indices derived by Parton et al. (1988) for the two processes.

The influence of soil water status on nitrification and denitrification has been documented by many authors (Mosier and Parton, 1985; Klemedtsson et al., 1988; Groffman and Tiedje, 1988). Aerobic microbial activity increases with soil water content until a point is reached where water displaces air and restricts oxygen diffusion. Maximum rates of nitrification occur at the highest water content at which soil aeration remains nonlimiting, with SWC ~60–80% of SSC. And so we assigned maximum nitrification potential WATER at SWS around 6–8 (Table 2).

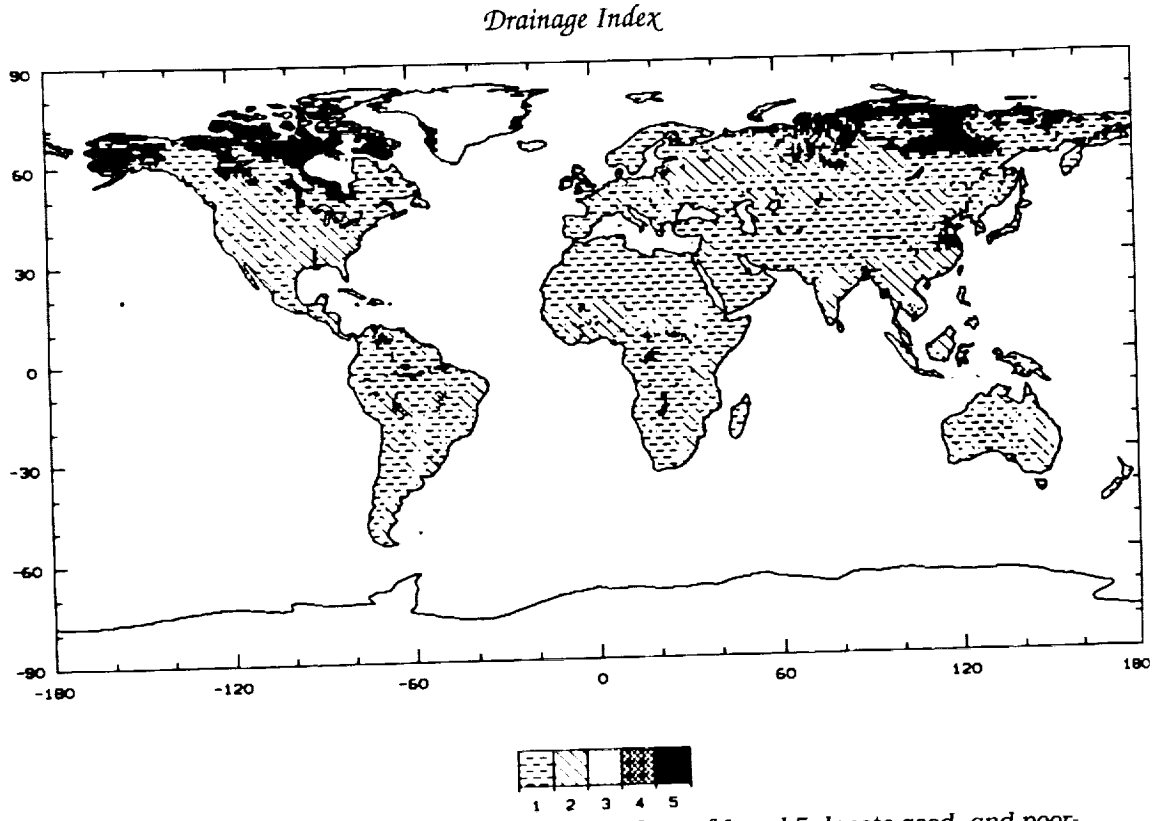

Figure 6. Distribution of the drainage index DRNG. Values of 1 and 5 denote good- and poor-drainage soils, respectively.

Table 1: Soil water status, as a function of the soil drainage scale and calculated soil water content/soil water storage capacity

SWC/SSC (%)	Drainage Scale				
	1	2	3	4	5
0 - 20	1	1	1	1	2
20 - 30	2	2	2	2	3
30 - 40	3	3	3	4	5
40 - 50	4	4	4	5	7
50 - 60	5	5	5	6	8
60 - 70	6	6	6	7	9
70 - 80	6	7	7	8	9
80 - 90	7	7	8	9	10
90 -100	7	8	9	10	10
>100%	8	9	10	10	10

Table 2: Water availability as a function of soil water status in current and preceding months

SWS, preceding month	SWS, current month									
	1	**2**	**3**	**4**	**5**	**6**	**7**	**8**	**9**	**10**
1	1	2	4	6	9	10	10	10	6	1
2	1	1	3	5	8	9	10	10	6	1
3	1	1	2	4	7	8	9	10	5	1
4	1	1	2	4	7	8	8	8	4	1
5	1	1	2	4	6	7	7	7	3	1
6	1	1	2	4	6	7	7	6	2	1
7	1	1	2	4	6	7	7	6	2	1
8	1	1	2	4	5	6	6	5	2	1
9	1	1	2	3	4	6	6	4	2	1
10	1	1	2	3	4	5	6	4	2	1
No dependence*		1	2	3	5	7	10	10	5	21

*Scalars depend only on the SWS in the current month.

The maximum N_2O production by nitrifier denitrification is between 80 and 100% water-holding capacity, while the peak for respiratory denitrifier N_2O production may be at water contents exceeding 100% water-holding capacity (Klemedtsson et al., 1988). Hence OXYGEN, the index of oxygen limitation and denitrification potential, was assigned a maximum value for SWS = 10 (Table 3).

Field measurements generally show high pulses of N_2O efflux from the soils after rainfall. Lacking any statistics, we do not know how significant these episodic pulses are in the global N_2O budget. Furthermore, there are presently no gridded climatologies of daily rainfall even for a continent. To test the importance of wetting and drying using the data available, we made the nitrification and denitrification indices dependent on the soil water status of the previous month in addition to the current month (see Tables 2 and 3). We hypothesized that dry soils that are wetted (large difference in SWS between previous and current months) are more favorable for N_2O production than soils with constant SWS. In this way, pulses of N_2O at the onset of a wet season would give a higher average monthly N_2O flux than in wet months preceded by moist conditions. The hysteresis effect observed (Groffman and Tiedje, 1988) is included by making the indices under drying conditions lower than those under equal amounts of wetting. This procedure imposes a one-month memory on the system, and the memory is probably much longer than that represented in the episodic pulses observed. This is thus one of the most uncertain aspects of the toy model, but an aspect that can be tested with long time-series measurements such as that of Parton et al. (1988).

Table 3: Oxygen limitation as a function of soil water status in current and preceding months

SWS, preceding month	SWS, current month 1	2	3	4	5	6	7	8	9	10
1	1	1	1	4	6	8	10	10	10	10
2	1	1	1	4	6	8	10	10	10	10
3	1	1	1	3	5	7	9	10	10	10
4	1	1	1	3	4	6	8	9	10	10
5	1	1	1	2	3	5	7	8	9	10
6	1	1	1	1	2	4	6	7	8	9
7	1	1	1	1	2	3	5	6	7	8
8	1	1	1	1	2	3	4	5	6	7
9	1	1	1	1	2	3	4	5	6	7
10	1	1	1	1	2	3	4	5	6	7
No dependence*	1	2	2	3	3	4	5	6	8	10

*Scalars depend only on the SWS in the current month.

In the reference case for N_2O production (see "N_2O Production"), we included the WATER and OXYGEN dependence on the water status of the previous month.

Soil Fertility

The last control on N_2O production we need to quantify is soil fertility. Matson and Vitousek (1987, 1990) have shown a strong relationship between N_2O flux and soil fertility in the tropics and subtropics, and that relationship is useful for regional estimation of N_2O emission. In this study, soil fertility for each of the 106 soil units was ranked subjectively based on general understanding of the cation exchange capacity and other soil properties. Because we did not feel that we were capable of distinguishing as many as ten levels of soil fertility, five ranks were used. A high value denotes a fertile soil, conducive to high levels of N_2O production. For example, Ferralsols, occurring mainly in the tropics, are strongly leached soils and their fertility is low because of their low cation exchange capacity, presence of alumina on the exchange complex, low content of weatherable minerals, and phosphorus fixation. A rank of 1–2 was assigned. In contrast, Chernozems and Kastanozems, underlying much of the agricultural lands in midlatitudes, are fertile soils to which a rank of 5 is assigned. The global distribution of the index FERT is shown in Figure 7.

N_2O Production

With the controls on N_2O fluxes quantified, it remains to combine them to yield PROD, the nondimensional index of N_2O production.

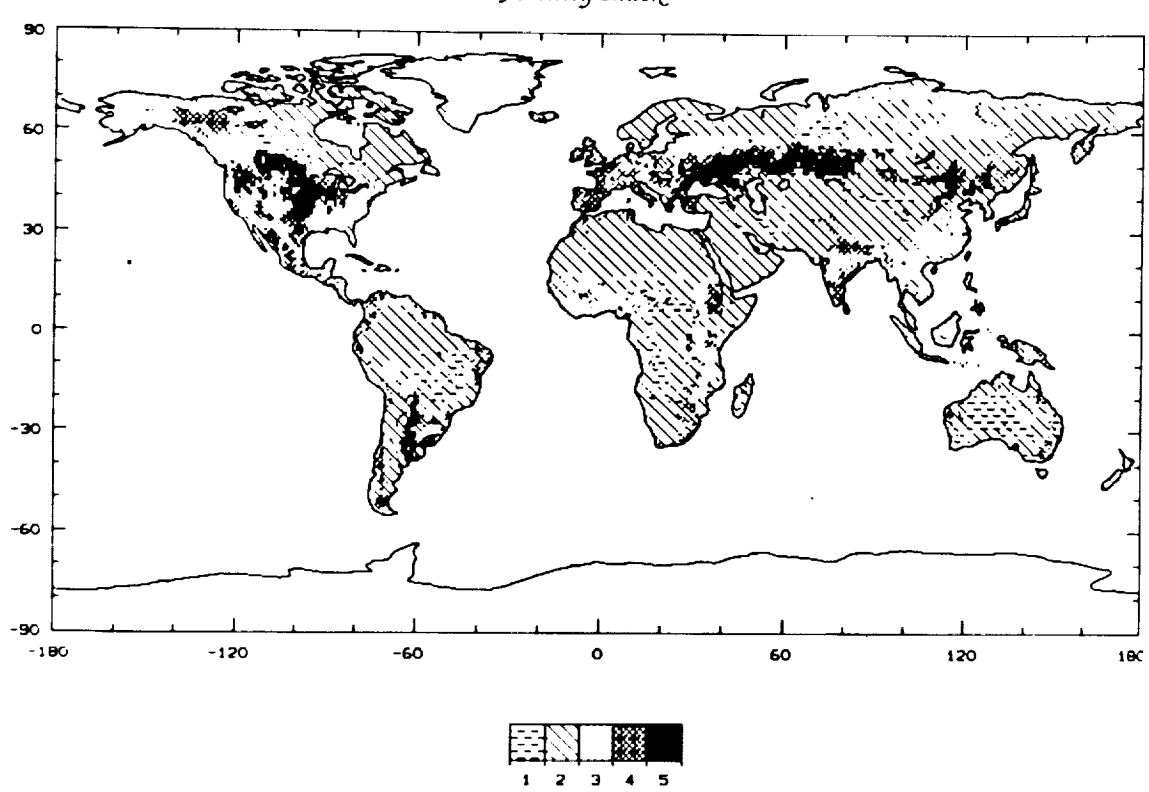

Figure 7. Distribution of the fertility index FERT. High values denote fertile soils, conducive to N_2O production.

We note that the five factors chosen are not independent. In particular, CARBON, scaled from the annual NDVI integral, captures geographic variations in temperature and soil moisture, as well as variations in soil fertility. While it may be argued that annual N_2O production may be proportional to CARBON alone, we still need to obtain seasonal variations in the production.

There are many ways to combine the factors. Lacking any global information, we first assumed that all five controlling factors are of equal importance, i.e., the maximum fertility factor has the same effect as the maximum oxygen limitation factor as far as N_2O production is concerned. Hence, although FERT was scaled from 1 to 5 because of our inability to discriminate further, FERT was multiplied by two to normalize to the other factors. The effects of the five factors may not be equal and can be analyzed in sensitivity analyses.

We then modeled the nondimensional N_2O production every month as the geometric mean of all five controlling factors. We

chose a geometric mean rather than an arithmetic mean because a factor of zero, such as when temperature falls below 0°C, automatically shuts down N_2O production. Also, a low value for one of the factors would lower the N_2O production index. For example, values of 1 and 9 for two factors are given less weight than 5 and 5, which yield the same arithmetic mean.

The degrees of nitrification and denitrification are both governed by the water and oxygen supply in the soil, and the products of nitrification provide the substrate for denitrification. However, the processes themselves are carried out by different microbial populations and are, to a large extent, independent of each other. It is thus not correct to multiply the denitrification and nitrification indices OXYGEN and WATER. In their model of N_2O production in the Colorado grasslands amended with urine, Parton et al. (1988) summed the contribution of the two processes to obtain the total N_2O production. There, sufficient data allowed the relative contributions of the processes to be obtained as a constant in the regression equation between the model and the flux measurements. Parton et al. found that nitrification contributed 60–80% of the total flux. This is in sharp contrast to tropical soils where denitrification dominates (e.g., Matson and Vitousek, 1990). We do not have information on the relative importance of nitrification and denitrification for all ecosystems, nor do we have sufficient N_2O flux measurements to carry out a regression analysis similar to that of Parton et al. (1988). Thus, this version of the toy model cannot discriminate between N_2O produced via the different processes, and the product of OXYGEN and WATER can only be viewed as an index of the total production.

The monthly N_2O production index, PROD, is calculated as follows in the reference case:

$$\mathrm{PROD} = [\mathrm{OXYGEN} \times \mathrm{WATER} \times \mathrm{SOD} \times \mathrm{FERT}^* \times \mathrm{CARBON}]^{1/5}$$

where PROD, OXYGEN, WATER and SOD are indices calculated monthly; FERT* = 2 × FERT; and CARBON has a fixed value for all months.

Model Evaluation

The model was applied at each of the 1° × 1° grid boxes for the globe, to yield, every month, the global variation of N_2O production. A series of sensitivity experiments was carried out. Instead of the reference exponential temperature dependence (SOD1), the quadratic (SOD2) and linear (SOD3) curves were used separately. Other sensitivity experiments selectively excluded each of the controlling factors.

Our next step is to compare our modeled indices for N_2O production from the reference case and each of the sensitivity experiments

with fluxes directly measured in the field. With the comparison, we hope to establish that the geographic and seasonal variations in the nondimensional N_2O indices capture those found in the field. We carried out a literature survey of measurements of N_2O fluxes from natural systems. Only six different ecosystems (wetlands, temperate forests, steppes, tropical savannas, tropical dry forests, and tropical rain forests) are represented. Some of the measurements spanned less than a month.

Where measurement conditions corresponded with the vegetation/soil/climate conditions in the digital data bases used as inputs to our toy model, we compared the measured N_2O flux and the modeled PROD, both averaged over the period of the measurements. For measurement sites where discrepancies exist between field conditions and model inputs, we recomputed PROD using the conditions of the measurement sites.

By averaging the data and model results over the period of measurements, we hope to ameliorate the impact of the phase errors associated with using surface air rather than soil temperatures in our analysis. Small-scale variability may still confound the comparison between point measurements and model calculations at 1° resolution. Ideally, we would average measurements in the 1° grid box for comparison. This being impossible, we averaged the modeled indices over a few grid boxes adjacent to the measurement sites, in hopes that variability within a grid box is reflected in variability among several grid boxes. A total of 30 data points resulted for the comparison.

Of all the sensitivity experiments, the standard model as presented above yielded the highest correlation coefficient. This is shown in Figure 8 together with the best line fit to the data. A quadratic fit

$$y = 78.9 - 52.3x + 12.4x^2$$

was found to produce the highest $r^2 = 0.57$ between the model and observations. Here x represents the modeled monthly averaged index PROD, and y the monthly averaged N_2O flux measured (g N/ha/mo).

Figure 9 shows the global distribution of PROD, summed over a year. The highest N_2O production is found in the equatorial regions where both temperature and NDVI exhibit their maximum values. In the reference case, the equatorial regions (30°N–30°S) account for 80% of the global production. While midlatitude Chernozems and Kastanozems have the highest fertility, and permafrost regions have highest oxygen limitation, their inclusion only reduces the latitudinal gradient in N_2O production.

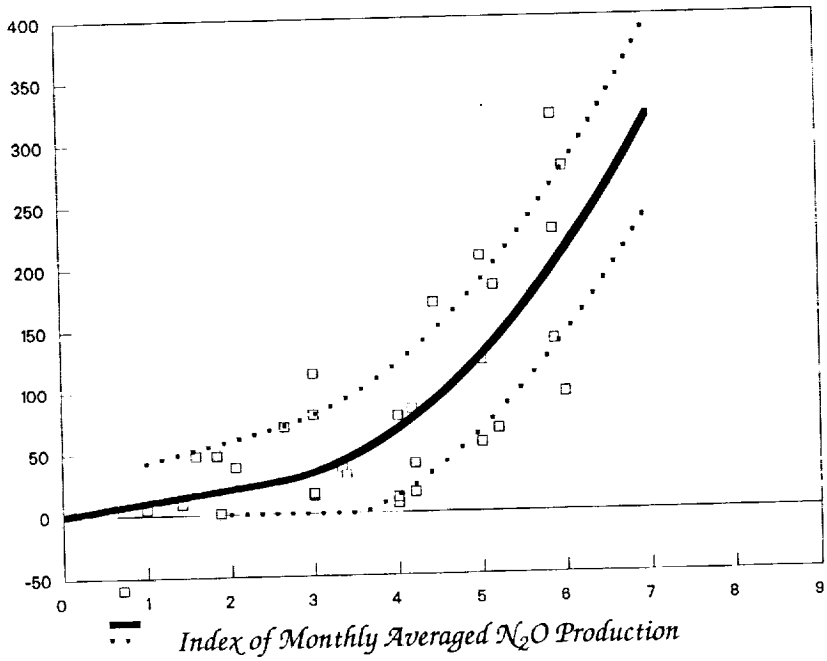

Figure 8. Comparison of PROD, the modeled N_2O index, with measured N_2O fluxes (boxes). The thick and dotted lines represent the best line fit ± 1 standard deviation.

Conclusion

The regression equation provides the transformation of the modeled nondimensional N_2O indices into dimensional N_2O fluxes. The global N_2O emission from natural soils obtained is 7 Tg N/yr (with a confidence interval of 3.1 to 13.4 Tg/yr). That our modeled estimate is within previous estimates for this source should be no surprise, as all extrapolation schemes are based on the same limited set of measurements of N_2O fluxes. Of the ~15,000 1° × 1° ice-free land cells, only 30 are represented with measurements. Thus the toy model, while more elaborate, does not provide a more accurate estimate of the global N_2O emission than other extrapolation schemes. However, the model and the sensitivity experiments do present a framework for analyzing how different controls affect N_2O production in different regions and for identifying the gaps in our understanding of N_2O emissions from natural soils, as well as a strategy for measurements.

A major implication of the toy model is that the tropics account for >80% of the global emission, within the range inferred by Prinn et al. (1990) from the atmospheric N_2O distribution. The large tropical source, in our model, is a result of the equal weighting given to

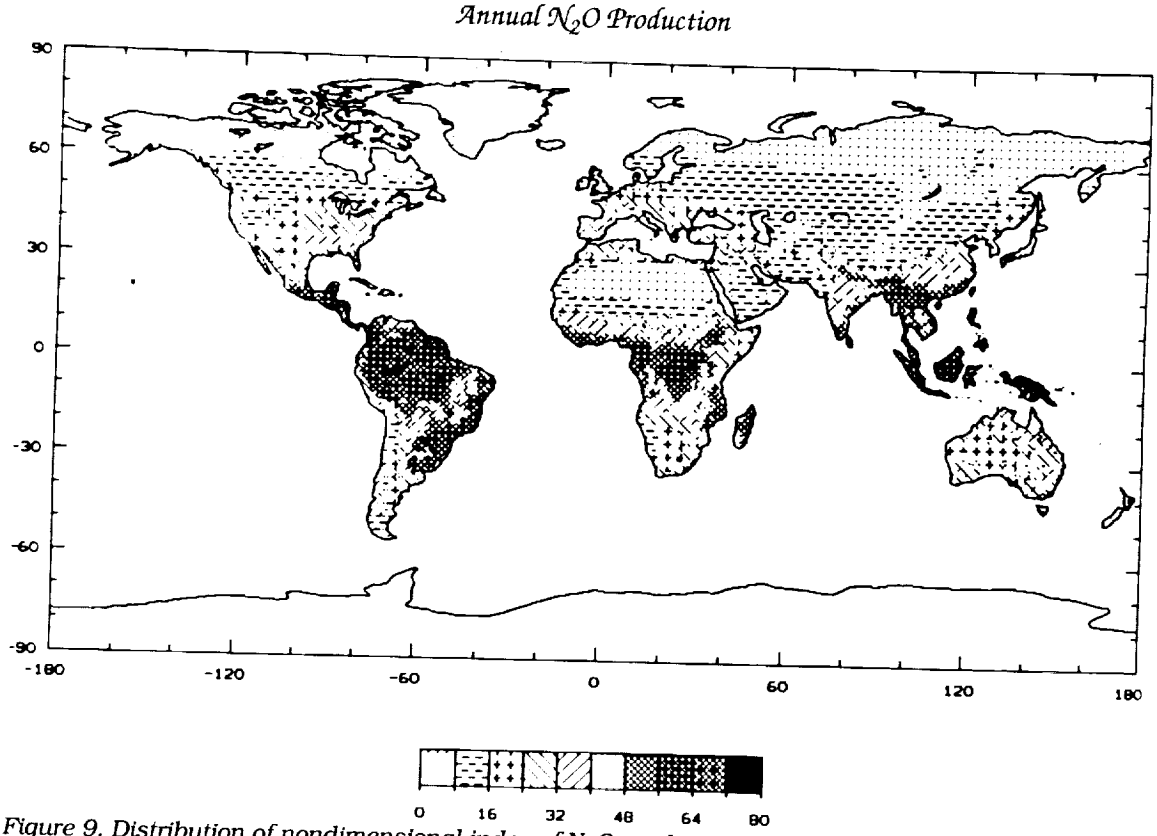

Figure 9. Distribution of nondimensional index of N_2O production, summed over the year.

the control factors. The latitudinal gradient in N_2O production is dominated by the controlling factors CARBON (carbon and nitrogen availability, proportional to NDVI) and SOD (decomposition rates, proportional to temperature). The two moisture indices for nitrification (WATER) and denitrification (OXYGEN) show no distinctive latitudinal gradients, while soil fertility peaks in the Chernozems and Kastenozems of midlatitudes. Whether the latitudinal gradient of N_2O production is as steep as that estimated by the toy model can be assessed by a detailed comparison and analysis of flux measurements from different locations.

We note Matson and Vitousek (1990) appear to have a significantly lower emission from the tropics than that estimated by the toy model. The difference may not be real, but may lie in the choices of areas or soil types included in the two calculations or in land use effects not included in this study. With the series of geographic data bases used in the toy model, it is straightforward to carry out parallel analyses so that the discrepancies can be evaluated and understood.

Improvement of the global estimate of N_2O emission from natural soils clearly requires more flux measurements. The toy model suggests that measurements should span at least a complete annual cycle, and should be carried out along several transects that cover different gradients in temperature, precipitation, soil texture and fertility, and vegetation productivity. It is also clear that complete site description, with soil, vegetation, and climatic data, is crucial for understanding the controls on N_2O production.

References

Bouwman, L., I. Fung, E. Matthews, and J. John. On the global distribution of N_2O emission from natural soils (in preparation).

Bowden, W.B. 1986. Gaseous nitrogen emissions from undisturbed terrestrial ecosystems: An assessment of their impacts on local and global nitrogen budgets. *Biogeochemistry* 2, 249–279.

Box, E.O., B.N. Holben, and V. Kalb. 1989. Accuracy of the AVHRR vegetation index as a predictor of biomass, primary productivity and net CO_2 flux. *Vegetatio 80*, 71–89.

Dickinson, R.E. 1984. Modeling evapotranspiration for three-dimensional global climate models. In *Climate Processes and Climate Sensitivity* (J.E. Hansen and T. Takahashi, eds.), Geophysical Monograph 29, American Geophysical Union, Washington, D.C., 58–72.

Dickinson, R.E., A. Henderson-Sellers, P.J. Kennedy, and M.F. Wilson. 1986. *Biosphere-Atmosphere Transfer Scheme (BATS) for the NCAR Community Climate Model.* Technical Note TN-275+STR, National Center for Atmospheric Research, Boulder, Colorado, 69 pp.

Elkins, J.W., T.M. Thompson, B.D. Hall, K.B. Egan, and J.H. Butler. NOAA/GMCC halocarbons and nitrous oxide measurements at the South Pole. *Antarctic Journal of the United States*, in press.

FAO-Unesco. 1971–1982. *Soil Map of the World*, 1:5000000, Vol. II-X, FAO, Rome, Italy.

FAO-Unesco. 1974. *Soil Map of the World*, Volume I, Legend. FAO, Rome, Italy.

FAO-Unesco. 1988. *Soil Map of the World. Revised Legend.* World Resources Report 60, FAO, Rome, Italy.

Firestone, M.K., and E.A. Davidson. 1989. Microbiological basis of NO and N_2O production and consumption in soil. In *Exchange of Trace Gases between Terrestrial Ecosystems and the Atmosphere* (M.O. Andreae and D.S. Schimel, eds.), John Wiley and Sons, Chichester, England, 7–21.

Fung, I.Y., C.J. Tucker, and K.C. Prentice. 1987. Application of Advanced Very High Resolution Radiometer Vegetation Index to study atmosphere-biosphere exchange of CO_2. *Journal of Geophysical Research 92*, 2999–3015.

Goward, S.N., C.J. Tucker, and D.G. Dye. 1986. North American vegetation patterns observed with the NOAA-7 advanced very high resolution radiometer. *Vegetatio 64*, 3–14.

Groffman, P.M., and J.M. Tiedje. 1988. Denitrification hysteresis during wetting and drying cycles in soil. *Soil Science Society of America Journal 52*, 1626–1629.

Hao, W.M., S.C. Wofsy, M.B. McElroy, J.M. Beer, and M.A. Toqan. 1987. Sources of atmospheric nitrous oxide from combustion. *Journal of Geophysical Research 92*, 13345–13372.

Houghton, J.T., G.J. Jenkins, and J.J. Ephraums (eds.). 1990. *Climate Change: The IPCC Scientific Assessment.* Intergovernmental Panel on Climate Change and Cambridge University Press, Cambridge, 329–341.

Klemedtsson, L., B.H. Svensson, and T. Rosswall. 1988. Relationships between soil moisture content and nitrous oxide production during nitrification and denitrification. *Biology and Fertility of Soils 6*, 106–111.

Manabe, S. 1969. Climate and ocean circulation. Part I: The atmospheric radiation and the hydrology of the earth's surface. *Monthly Weather Review 93*, 739–774.

Matson, P.A., and P.M. Vitousek. 1987. Cross-ecosystem comparisons of soil nitrogen and nitrous oxide flux in tropical ecosystems. *Global Biogeochemical Cycles 1*, 163–170.

Matson, P.A., and P.M. Vitousek. 1990. Ecosystem approach to a global nitrous oxide budget. *Bioscience 40*, 667–672.

Matthews, E. 1983. Global vegetation and land use: New high-resolution data bases for climate studies. *Journal of Climate and Applied Meteorology 22*, 474–487.

Mintz, Y., and Y. Serafini. 1981. *Global Fields of Soil Moisture and Land Surface Evapotranspiration.* Technical Memorandum 83907, Research Review 1980/81, NASA Goddard Flight Center, 178–180.

Mosier, A.R., and W.J. Parton. 1985. Denitrification in a shortgrass prairie: A modeling approach. In *Planetary Ecology* (D.E. Caldwell, J.A. Brierley, and C.L. Brierley, eds.), Van Nostrand Reinhold Co., New York, 441–451.

Muzio, L.J., and J.C. Kramlich. 1988. An artifact in the measurement of N_2O from combustion sources. *Geophysical Research Letters 15*, 1369–1372.

Parton, W.J., A.R. Mosier, and D.S. Schimel. 1988. Rates and pathways of nitrous oxide production in a shortgrass steppe. *Biogeochemistry 6*, 45–48.

Parton, W.J., D.S. Schimel, C.V. Cole, and D.S. Ojima. 1987. Analysis of factors controlling soil organic matter levels in Great Plains grasslands. *Soil Science Society of America Journal 51*, 1173–1179.

Prinn, R.G., D. Cunnold, R. Rasmussen, O. Simmonds, F. Alyea, A. Crawford, P. Fraser, and R. Rosen. 1990. Atmospheric trends and emissions of nitrous oxide deduced from ten years of ALE-GAGE data. *Journal of Geophysical Research 95*, 18369–18385.

Seiler, W., and R. Conrad. 1987. Contribution of tropical ecosystems to the global budgets of trace gases, especially CH_4, H_2, CO and N_2O. In *Geophysiology of Amazonia* (R.E. Dickinson, ed.), John Wiley & Sons, New York, 133–162.

Sellers, P.J., Y. Mintz, Y.C. Sud, and A. Dalcher. 1986. A simple biosphere model (SiB) for use within general circulation models. *Journal of the Atmospheric Sciences 43*, 505–531.

Shea, D.J. 1986. *Climatological Atlas 1950–1979: Surface Air Temperature, Precipitation, Sea-Level Pressure and Sea Surface Temperature (45°S–90°N)*. Technical Note NCAR/TN-269+STR, National Center for Atmospheric Research, Boulder, Colorado.

Tarpley, J.D., S.R. Schneider, and R.L. Money. 1984. Global vegetation indices from the NOAA-7 meteorological satellite. *Journal of Climate and Applied Meteorology 23*, 491–494.

Thornthwaite, C.W. 1948. An approach toward a rational classification of climate. *Geographical Review 38*, 55–74.

Zobler, L. 1986. *A World Soil File for Global Climate Modeling*. NASA Technical Memorandum 87802, NASA, New York, 32 pp.